Desalination and Water Treatment
www.deswater.com
doi: 10.5004/dwt.2020.24971

178 (2020) 387–395
February

A novel and facile antibacterial sponge for effective demulsification and oil/water emulsions separation

Jeng-Yi Wu, Chao-Wei Huang, Ping-Szu Tsai*

Department of Chemical and Materials Engineering, National Kaohsiung University of Science and Technology, No. 415, Jiangong Rd., Sanmin Dist., Kaohsiung City 80778, Taiwan, R.O.C., Tel. +886-7-3814526 Ext: 15139; emails: charles1@nkust.edu.tw (P.-S. Tsai), supershatman@gmail.com (J.-Y. Wu), Tel. +886-7-3814526 Ext: 15135; email: huangcw@nkust.edu.tw (C.-W. Huang)

Received 17 May 2019; Accepted 25 September 2019

ABSTRACT

A novel underwater superoleophobic sponge for emulsion wastewater treatment was fabricated by [3-(methacryloylamino)propyl]trimethylammonium chloride polymer. The emulsion separation efficiency, antibacterial ability, and the mechanism of the automatic demulsification phenomenon of the prepared sponge were investigated. The experimental results showed that the sponge exhibited the property of underwater superoleophobicity and its separation efficiencies for separating oil/water emulsions of chloroform, heptane, kerosene, toluene, and vegetable oil were above 99%. Besides, the sponge's antibacterial efficiency was above 99% for *Escherichia coli* and *Staphylococcus aureus*. In addition, the prepared sponge had high sodium dodecyl sulfate (SDS) adsorption ability; therefore, it could change the ionic balance of the emulsions stabilized by SDS. The destroyed emulsions would be aggregated to form large but unstable emulsions. Consequently, these unstable emulsions would be separated, leading to the formation of the oil layer. This schematic mechanism of the automatic demulsification phenomenon was also proposed in this study.

Keyword: [3-(Methacryloylamino)propyl]trimethylammonium chloride; Emulsion separation; Demulsification; SDS adsorption; Antibacterial property; Underwater superoleophobic

1. Introduction

Wastewater containing emulsified oil-water mixtures had been produced in many industries, including petrochemicals, food, textiles, leather, and the surface treatments of steel and metals [1–5]. Besides, many emulsion effluents containing surfactants also had been used in shale oil mining technology. The effective recovery or separation of these emulsions would exhibit a significant economic impact [6–8]. However, the separation of the emulsified oil-water mixtures was difficult and became a global challenge.

Conventional techniques such as skimmers, centrifuges, coalescers, sedimentation tanks, depth filters, magnetic separation, and flotation techniques could be used to separate immiscible oil-water mixtures, but not suitable for stable oil/water emulsions [9,10]. Additionally, emulsions with micron and submicron-sized droplets required a long residence time for gravity separation. Even the addition of chemicals could not effectively destroy those stable emulsions. Therefore, in order to solve these issues, various demulsification processes have been developed in literatures to solve the problem of emulsion wastewater, such as chemical demulsification [11–13], centrifugation [14,15], thermal treatment [16–18], electrical demulsification [19,20], ultrasonic demulsification [21–23] and biological demulsification [24,25]. However, these conventional methods could not extract water with the oil concentration lower than 1 vol.% of the total wastewater. On the other hand, the oil droplets below 10 μm could not be removed efficiently either [26,27].

To overcome these issues, membrane separation technology was an alternative method [28–31], which was

* Corresponding author.

initially used to reverse osmosis [32], membrane distillation [33], microfiltration [34,35], and ultrafiltration [36,37]. The performance of the membrane was significantly affected by the surface properties, such as wettability, surface charge, pore size, and roughness [38–40]. During the membrane separation process for the emulsions, the charge interaction between the emulsions and the membrane surface would facilitate the fragmentation and coagulation of the emulsions [41,42]. According to this previous literature, a positive-charged surface would facilitate demulsification for the emulsions synthesized by a negative surfactant [43,44]. Therefore, it could conclude that while an emulsion separation membrane had a positive-charged surface, the separation efficiency of the membrane could be improved.

For example, Xu et al. [45] used the chitosan-polyacrylamide sponge to achieve the emulsion demulsification by the extrusion method effectively. Wu et al. [46] investigate the influence of surface charge on emulsion separation and demulsification. Both references implied that the cationic support had exhibited a better emulsion separation performance than the anionic one. On the other hand, an extrusion or filtration process was necessary to achieve the demulsifying effect of the emulsion. In spite of the above results, the automatic demulsification phenomenon has never been proposed and the possible effects of bacteria on the support [47–50] have not to be investigated.

In our previous study [51], we had synthesized the quaternary ammonium salt polymer mesh membrane with a high separation efficiency (>99%), high permeate flux (up to 4,308 L h^{-1} m^{-2}), durability (up to 120 times), and good anti-bacterial property to separate oil-water mixtures. However, the efficiency of separating oil/water emulsions needs to be improved. In this study, we proposed a novel and facile sponge, which was synthesized by using a quaternary ammonium salt polymer. The separation efficiency of emulsions, antibacterial ability, and the mechanism of the fantasy automatic demulsification process were investigated. In addition, the surface morphology, the wetting characteristics, the surfactant adsorption characteristics, and the separation efficiency of various oil/water emulsions of the sponge would be discussed.

2. Materials and experimental methods

2.1. Materials

[3-(Methacryloylamino)propyl]trimethylammonium chloride solution (MAPTAC, 50%) was chosen as the monomer with the crosslinking agent of N,N′-Methylenebisacrylamide (MBA, ≥99%) to synthesize the polymer materials. The ammonium persulfate (APS, ≥95%) was employed as the initiator in the polymerization. All chemicals mentioned above were obtained from Sigma-Aldrich (St. Louis, MO, USA). Various substrates for the prepared polymers were listed below. First, stainless steel mesh with a pore size of 45 μm was purchased from Yung Sheng Wire Co. Ltd., (Taichung, Taiwan). Second, melamine sponge was obtained from Litai Plastic Industry Co. Ltd., (Taiwan) and thirdly polyvinyl alcohol (PVA) sponge was bought from Speed International Research Co. Ltd., (Taichung, Taiwan). On the other hand, sodium dodecyl sulfate (SDS) was an ionic surfactant to be employed as an emulsifier for preparing the oil/water emulsions. The oil sources of the emulsions could be chloroform (First grade), toluene (First grade), heptane (≥99%), vegetable oil, and kerosene. SDS, chloroform, and toluene were purchased from Nihon Shiyaku Co. Ltd., (Japan) and heptane was bought from Sigma-Aldrich as well. The vegetable oil was provided from Standard Food Corporation (Taipei, Taiwan) and kerosene was obtained from Chinese Petroleum Corporation (Taiwan).

2.2. Preparation of polymer solutions

For the polymerization process, monomers (20 g of MAPTAC), a crosslinking agent (0.1 g of MBA), and an initiator (0.5 g of APS) were dissolved in deionized water by stirring for 1 h. The polymer solution was used as the coating material for preparing the oil/water emulsion separation sponges.

2.3. Preparation of polymer-coated oil-water separation sponge

The as-prepared polymer solution was deposited on various substrates by the dip-coating method, including cleaned stainless steel meshes, melamine sponges, and PVA sponges. As shown in Fig. 1a, these substrates were immersed in the polymer solution and then drawn horizontally. Subsequently, the polymer-coated substrates were heated in an oven at 85°C for 180 min. The schematic diagram of the polymerization reaction is represented in Fig. 1b. For the sake of removing the nonreactive monomers, the polymer-coated sponges or meshes were flushed by deionized water after polymerization. Consequently, the oil/water emulsion separation sponges were prepared and their emulsion separation efficiencies, demulsification property, and antibacterial property would be examined.

2.4. Emulsion separation test

The oil/water emulsions were prepared by emulsifying water and various oil sources in 5 vol.%. The oil sources included chloroform, heptane, toluene, kerosene, and vegetable oil. With the addition of 1 mg mL^{-1} of SDS emulsifier, the polymer solutions were operated under a homogenizer at 10,000 RPM for 5 min. The sizes of emulsions mentioned above were controlled in a range of 0.5–2 μm, measured by a dynamic light scattering particle size analyzer (BIC 90 Plus, Brookhaven, U.S.). Before the oil/water emulsions separation experiment, the prepared sponges were pre-wetted in water for 10 min and then mounted onto the separation apparatus, as shown in Fig. 1c. Under the vacuum pressure of 0.1 MPa, emulsions started to be separated and the filtrate was collected in the flask. The separation efficiency could be represented by the oil rejection coefficient R (%) [52]:

$$R(\%) = \left(1 - \frac{C_p}{C_0}\right) \times 100\% \quad (1)$$

where C_0 and C_p were the oil concentration of the oil/water emulsion before and after separation, respectively.

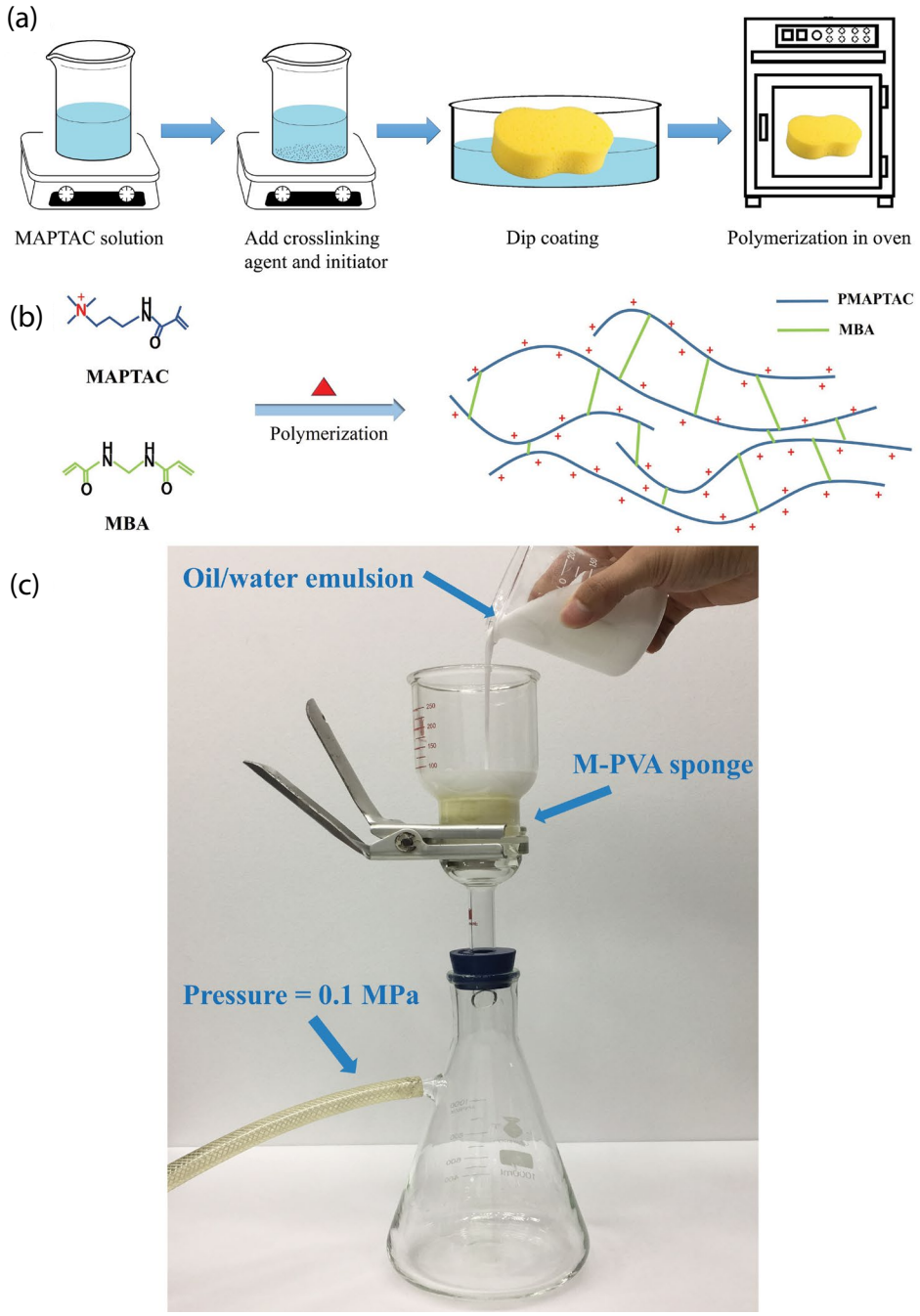

Fig. 1. (a) Schematic diagram of preparing oil/water emulsion separation sponges, (b) the schematic diagram of the polymers cross-linking reaction, and (c) the apparatus for oil/water emulsion separation.

2.5. Demulsification experiment

The anionic surfactant-stabilized oil/water emulsion was synthesized by emulsifying 50 vol.% oil source (such as chloroform, heptane, toluene, kerosene, and vegetable oil) with deionized water by using a surfactant of 1 mg mL^{-1} SDS in a beaker. The synthesized emulsion was poured into a test tube, and then the as-prepared sponge was immersed into the emulsion. Subsequently, the changes in the emulsion would be recorded over time.

2.6. SDS adsorption test

The SDS adsorption ability of prepared polymer was verified by the following processes. Initially, the polymer solution was heated in an oven at 85°C for 180 min to get the dry polymer. 1 g dry polymer was added into a 100 mL SDS solution with a concentration of 5,000 ppm in a beaker. Then the change in SDS concentration from 0 to 180 min was measured. The SDS adsorption ratio was defined as the following equation:

$$\text{SDS adsorption ratio}(\%) = \left(1 - \frac{C_t}{C_i}\right) \times 100\% \quad (2)$$

where C_i and C_t were the initial SDS concentration and the SDS concentration at time t (min), respectively. The analysis of SDS concentration was assessed by referring to Standard Methods (5540C) [53,54]. The 5540C method is followed by the mechanism that anionic surfactant could be bound to methylene blue (cationic dye) by the electrostatic force to become methylene blue active substance (MBAS). The MBAS in the aqueous phase would be extracted into the organic phase by using chloroform. Then the concentration of MBAS was determined by the absorbance at 652 nm which was measured by using a spectrophotometer. Consequently, the concentration of the anionic surfactant was quantified.

2.7. Antibacterial test

The antibacterial activity was examined according to the standard shake flask method (ASTM-E2149-01) [55,56]. This method provided the quantitative data by the average colony-forming units per milliliter (CFU mL^{-1}) of buffer solution in the flask. For measuring the antibacterial reduction rate of the prepared polymer, *Escherichia coli* (*E. coli*) (ATCC 23815) and *Staphylococcus aureus* (*S. aureus*) (ATCC 21351) were used as the model bacteria because of their easy reproduction in water widely. In the beginning, the target *E. coli* or *S. aureus* was cultured in Luria–Bertani broth at 37°C for 24 h to reach mid-log phase, and then the bacterial suspension was diluted with a 0.9% NaCl solution at pH 6.5 to the cell concentration of 10^6–10^7 CFU mL^{-1}. Additionally, a 5 mL diluted solution was withdrawn and incubated with immersing a piece of polymer-coated sponge (10 mm × 10 mm) within a test tube at 37°C. To determine the inoculum cell density, the suspensions were withdrawn before contacting with the polymer-coated sponge as well as the samples after contacting in 1 h. The withdrawn suspensions were diluted serially in the sterile buffer solution, spread on a nutrient plate count agar (PCA), and further incubated at 37°C for 24 h to determine the quantities of surviving bacteria. By counting the number of colonies, the antibacterial rate was defined as follows:

$$\text{AR} = \left(\frac{n_0 - n}{n_0}\right) \times 100\% \quad (3)$$

where n_0 and n are the average number of bacteria before and after contacting with the dilute samples, respectively. All experiments were repeated three times to confirm reliability.

Additional, the antibacterial property of the polymer-coated sponge was tested by the inhibition zone method [57]. In this method, *E. coli* and *S. aureus* were taken as the model bacteria as well. Initially, the cell concentration of the model bacteria was controlled at 10^6–10^7 CFU mL^{-1}. Then the sponge was cut into small pieces and deposited on the plates with a nutrient PCA. The plates were examined for the formation of a possible clear zone after incubation at 37°C for 24 h. The presence of a clear zone around the piece sample was recorded as an inhibition zone against *E. coli* and *S. aureus*.

2.8. Other characterizations

The surface chemistry of resulting sponges was characterized by Fourier transform infrared spectroscopy (FTIR, BI0-RAD165, Perkin-Elmer, U.S.). To characterize the hydrophobicity of polymer-coated sponges, underwater oil contact angles were measured by using a contact angle meter (GBX-PX610, Germany). During the measurement, chloroform droplets (2 μL) were dropped carefully on the polymer-coated sponges underwater at the ambient temperature. The average contact angle was determined by measuring more than five different positions on the same sample. The images of the polymer-coated sponges were obtained from a scanning electron microscopy (SEM, JEOL-I6700, Japan) with an acceleration voltage of 15 kV and a magnitude of 1,000×.

3. Results and discussion

3.1. Characterization of MAPTAC polymer coating

To confirm the formation of the synthesized polymer, the FTIR spectroscopy was used to determine the characteristic absorption bands associated with functional groups of the quaternary ammonium salt monomers. As shown in Fig. 2, the broad peak around 3,457 cm^{-1} and the sharp peak at 2,873 cm^{-1} were assigned to the O–H and C–H stretching bands [58], respectively. The bending band of the quaternary ammonium groups ($-N^+(CH_3)_3$) was approximately at 1,483 cm^{-1} [59]. The absorption bands at 1,636 and 1,608 cm^{-1} were corresponding to the C=C groups of the monomer MAPTAC [58,60]. When MAPTAC was polymerized into a polymer, the conversion of the monomers tested by potassium permanganate titration exceeded 99% and the peak of C=C groups disappeared, indicating that MAPTAC was successfully polymerized. To confirm that the MAPTAC polymer coating was successfully coated on the surface of the melamine and PVA sponge substrates, the difference between these two substrates before and after the MAPTAC polymer-coated was examined by an SEM microscopy. Fig. 3 shows the SEM images of the melamine sponge (a) before and (b) after the

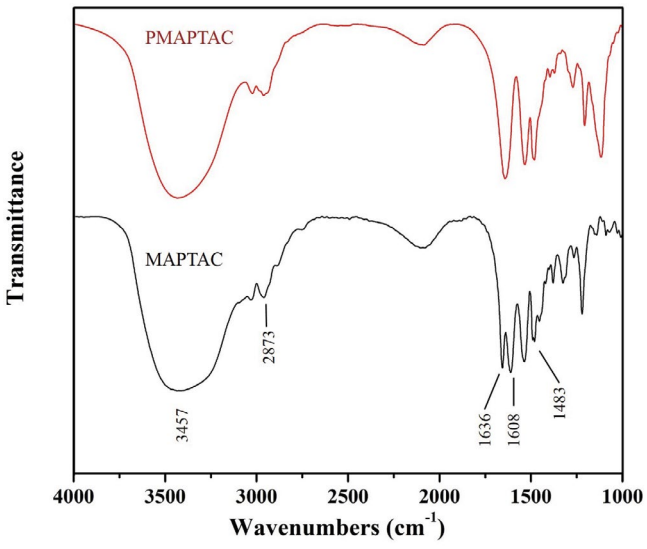

Fig. 2. FTIR spectrum before and after MAPTAC polymerization.

MAPTAC polymer was coated. It was observed that the initial pore size of the melamine sponge was about 50 μm. There was no noticeable change in the pore size after coating MAPTAC polymer, but it was observed that some of these pores were filled with MAPTAC polymers. Fig. 3 also shows the SEM images of the PVA sponge (c) before and (d) after coating MAPTAC polymer. The surface of the MAPTAC polymer-coated PVA sponge was transformed from a wrinkled grain to a smooth surface, indicating that the polymers were successfully coated on the surface of the PVA sponge.

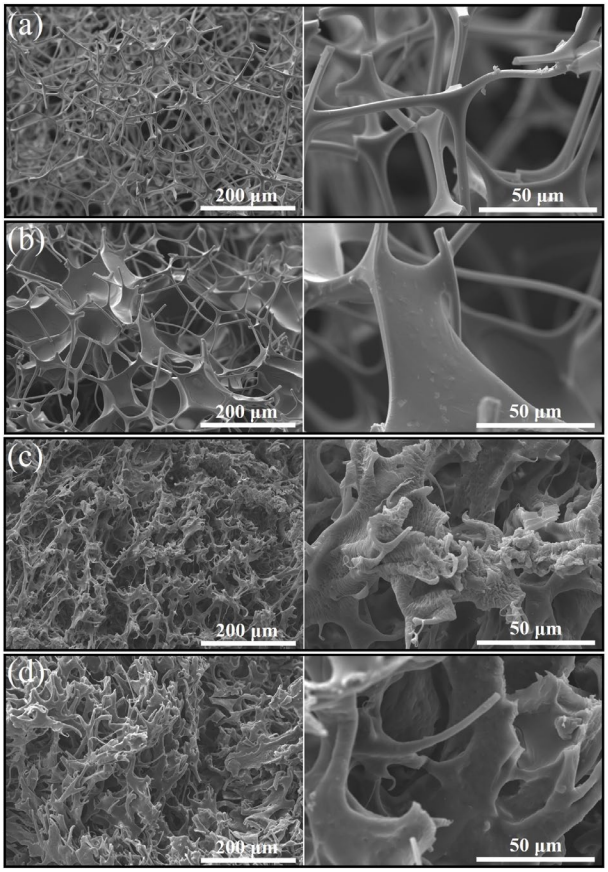

Fig. 3. SEM images of the melamine sponge (a) before and (b) after coating MAPTAC polymer; the PVA sponge (c) before and (d) after coating MAPTAC polymer.

3.2. Separation efficiency of MAPTAC polymer coating on various substrates

Fig. 4a shows the separation efficiency of the oil-water mixture and emulsion by using MAPTAC polymer coating on various substrates, including PVA (M-PVA) sponge, melamine (M-Me) sponge, and stainless steel (M-S) mesh. All polymer-coated substrates could effectively separate the oil-water mixture and their separation efficiency could be more than 99%. However, emulsion separation efficiencies were different while different substrates were used. Their emulsion separation efficiencies of M-PVA sponge, M-Me sponge, and M-S mesh were 99.8%, 83.9%, and 26.9%, respectively. Accordingly, the PVA sponge was the best choice to be served as the substrate for MAPTAC polymer coating. Subsequently, the emulsion separation efficiency and the underwater oil contact angle of the M-PVA sponge for various oil sources were discussed for comparison. As shown in Fig. 4b, the separation efficiencies of M-PVA sponge for chloroform, heptane, kerosene, toluene, and vegetable oil emulsions were 99.2%, 99.1%, 99.5%, 99.7%, and 99.2%, respectively. The underwater oil contact angles of M-PVA sponge for chloroform, heptane, kerosene, toluene, and vegetable oil were 152°, 152°, 150°, 159°, and 150°, respectively, indicating that the M-PVA sponge exhibited a distinct underwater superoleophobicity.

3.3. Demulsification of M-PVA

Moreover, the M-PVA sponge not only had excellent emulsion separation and underwater superoleophobic property but also possessed a considerable demulsification property. The M-PVA sponge could effectively demulsify the emulsion of 50 vol.% kerosene in water prepared by using

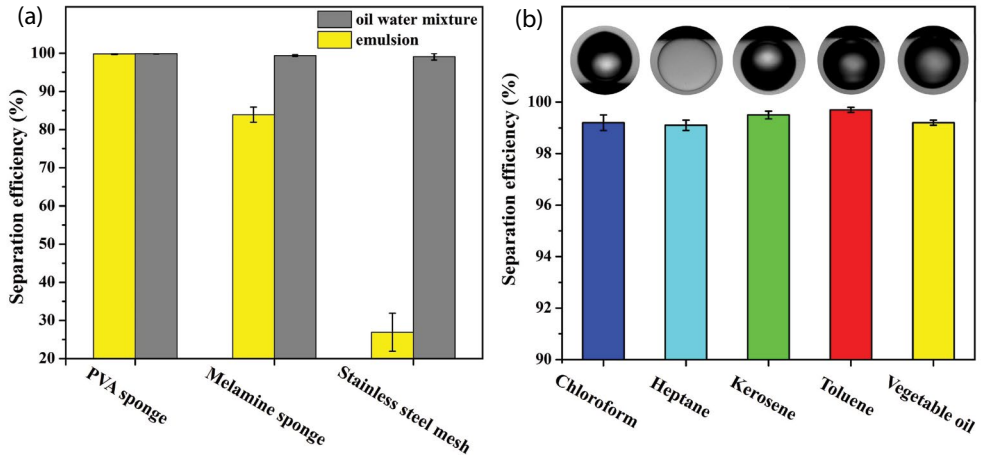

Fig. 4. (a) The separation efficiency of the oil water mixture and oil/water emulsion by using M-PVA, M-Me, and M-S substrates and (b) the separation efficiencies of various oil/water emulsions by using M-PVA sponge and their images of the underwater oil contact angle.

1 wt.% SDS as an emulsifier. When the M-PVA sponge was placed into the emulsion, the M-PVA sponge sank to the bottom of the emulsion. After about 20 s, a unique phenomenon of demulsification was observed. A small layer of oil suddenly appeared in the top layer of the stabilized emulsion. Meanwhile, many disturbances were continuously observed at the interface between the layered oil and emulsion. In addition, new droplets of oil appeared and started to aggregate, following by floating around the sponge. After 5 min, most of the emulsions were destroyed and a separate oil layer was formed. After 24 h, a distinctly separate oil layer and a demulsified water layer were observed, as shown in Fig. 5a. Additionally, no residual SDS was analyzed in the demulsified water layer. It indicated that most of the SDS were adsorbed on the M-PVA sponge to cause the demulsification. Besides the emulsion of kerosene in water, the M-PVA sponge can also effectively demulsify the emulsions of chloroform, heptane, toluene, and vegetable oil in water, as shown in Figs. 5b–e.

3.4. Verification of SDS adsorption on MAPTAC polymer

To verify the SDS adsorption on MAPTAC polymer, the SDS solution of 5,000 ppm was used to perform the adsorption test by using a pure MAPTAC polymer. As shown in Fig. 6, during the first 20 min of adsorption, the MAPTAC polymer rapidly absorbed 94.5% SDS. As time went on, the adsorption rate became slow and the SDS adsorption ratio reached almost 100% after 180 min. The calculated amount of saturated adsorption of MAPTAC to SDS was 1.3 g g^{-1}, which meant that the MAPTAC polymer had excellent adsorption ability of SDS.

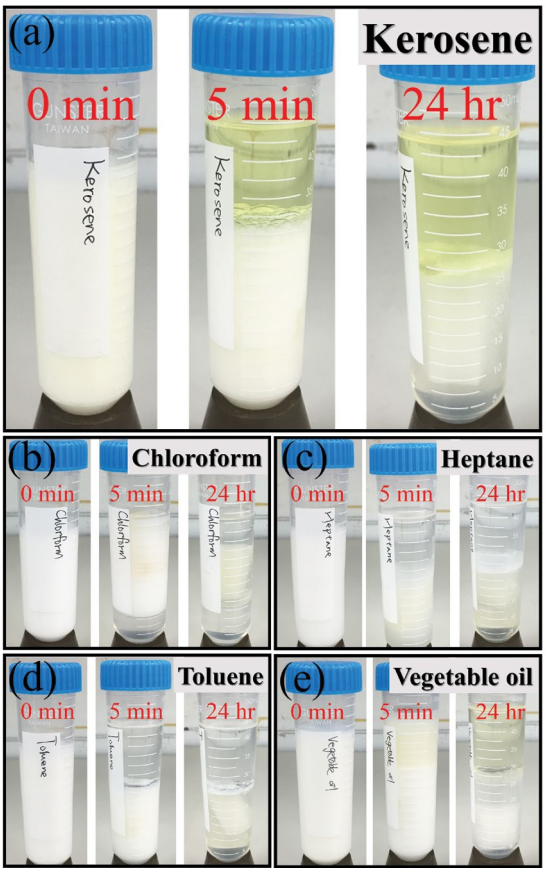

Fig. 5. Photographs of M-PVA sponge dampening in the emulsion of 50 vol.% (a) kerosene, (b) chloroform, (c) heptane, (d) toluene, and (e) vegetable oil in water by using 1% SDS as an emulsifier.

3.5. Demulsification mechanism of oil/water emulsion using the M-PVA sponge

Fig. 7 shows the demulsification mechanism of the M-PVA sponge for an oil/water emulsion with the SDS emulsifier. The negative charge of SDS would be drawn to the sponge due to the presence of the positive charge of the MAPTAC polymer. Therefore, the M-PVA sponge would adsorb the SDS, making the emulsions unstable. These unstable emulsions gradually aggregated together and formed the large emulsions. Due to the density differences

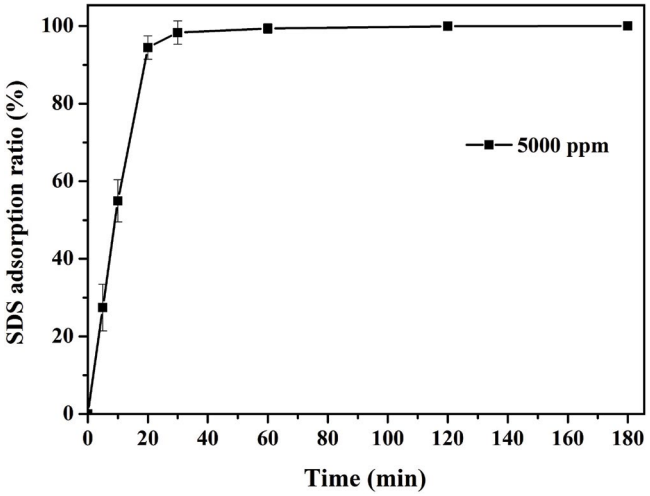

Fig. 6. SDS adsorption ratio on MAPTAC polymer with time.

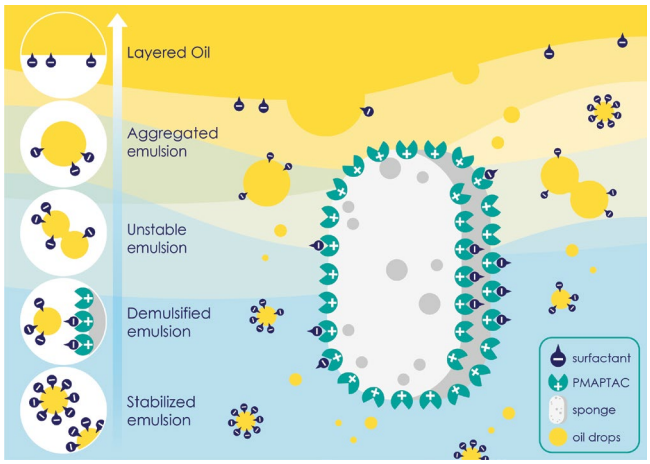

Fig. 7. Demulsification mechanism of oil/water emulsion using the M-PVA sponge.

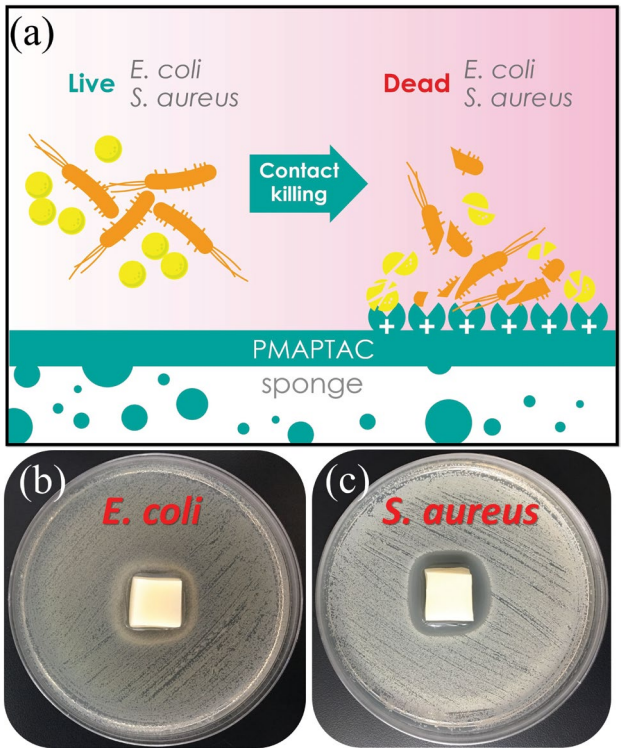

Fig. 8. (a) Schematic diagram of the antibacterial mechanism of M-PVA sponge; the inhibition zone of the M-PVA sponge against, (b) *E. coli*, and (c) *S. aureus*.

between large emulsions and water, the convection and diffusion phenomena of large emulsions on the surface were observed. These phenomena sustained, leading to the large emulsions ascending and accumulating into a continuous oil layer eventually.

3.6. Antibacterial properties of the M-PVA sponge

During the separation process of the emulsions, the bacteria were generally present and caused some adverse effects, such as increasing membrane filtration resistance, consuming energy, and reducing membrane performance and service life. Therefore, the emulsion separation membrane with antibacterial properties could improve the above problems. The material used in the experiment was a quaternary ammonium polymer with antibacterial properties. The antibacterial mechanism of M-PVA sponge is shown in Fig. 8a. The *E. coli* or *S. aureus* were easily adsorbed on the M-PVA sponge owing to the positive surface charge of the sponge. Sequentially, the internal charge balance of the bacterial cell wall would be destroyed, resulting in the death of the bacteria. Figs. 8b and c also show the apparent inhibition zone of M-PVA sponge against *E. coli* and *S. aureus*. In addition, when the antibacterial efficiency of the M-PVA sponge was tested by the standard shake flask method, the antibacterial efficiencies of *E. coli* and *S. aureus* were 99.30% and 99.99%, respectively, indicating that the prepared M-PVA sponge in this study had excellent antibacterial properties.

4. Conclusion

This study successfully produced a novel demulsification sponge for the treatment of various emulsified wastewaters. The demulsification sponges exhibited high emulsification separation efficiencies, high antibacterial activities, and individual demulsification performances. Based on the results of FTIR spectroscopy and SEM photograph, the MAPTAC polymer was successfully synthesized and coated on the surface of the sponge. The M-PVA sponge not only had excellent underwater superoleophobic properties but also achieved a separation efficiency of more than 99% for emulsions and oil-water mixtures. In addition, the M-PVA sponge had an excellent ability to absorb SDS, resulting in a good demulsification ability. Accordingly, the M-PVA sponge could effectively demulsify oil/water emulsions of chloroform, heptane, kerosene, toluene, and vegetable oil, leading to the formation of a water layer and an oil layer after demulsification. The proposed automatic demulsification mechanism showed that the M-PVA sponge would adsorb the SDS from the emulsions, resulting in the aggregation and accumulation of large emulsions droplets, following by the formation of a layered oil. On the other hand, the results of the antibacterial tests confirmed that the M-PVA sponge also had an excellent antibacterial property against *E. coli* and *S. aureus*. In summary, this study provided a new strategy and demulsification mechanism for the design of demulsified sponges and it could be expected to play an essential role in the treatment of emulsified wastewaters in the future.

References

[1] W.B. Zhang, Z. Shi, F. Zhang, X. Liu, J. Jin, L. Jiang, Superhydrophobic and superoleophilic PVDF membranes for effective separation of water-in-oil emulsions with high flux, Adv. Mater., 25 (2013) 2071–2076.
[2] B. Chakrabarty, A.K. Ghoshal, M.K. Purkait, Ultrafiltration of stable oil-in-water emulsion by polysulfone membrane, J. Membr. Sci., 325 (2008) 427–437.
[3] M.A. Shannon, P.W. Bohn, M. Elimelech, J.G. Georgiadis, B.J. Mariñas, A.M. Mayes, Science and technology for water purification in the coming decades, Nature, 452 (2008) 301.
[4] L.P. Gossen, L.M. Velichkina, Environmental problems of the oil-and-gas industry (Review), Petrol. Chem., 46 (2006) 67–72.
[5] A. Fakhru'l-Razi, A. Pendashteh, L.C. Abdullah, D.R.A. Biak, S.S. Madaeni, Z.Z. Abidin, Review of technologies for oil and gas produced water treatment, J. Hazard. Mater., 170 (2009) 530–551.
[6] B. Avvaru, N. Venkateswaran, P. Uppara, S.B. Iyengar, S.S. Katti, Current knowledge and potential applications of cavitation technologies for the petroleum industry, Ultrason. Sonochem., 42 (2018) 493–507.
[7] N. Pal, N. Saxena, A. Mandal, Studies on the physicochemical properties of synthesized tailor-made gemini surfactants for application in enhanced oil recovery, J. Mol. Liq., 258 (2018) 211–224.
[8] C.L. Chen, S.S. Wang, M.J. Kadhum, J.H. Harwell, B.-J. Shiau, Using carbonaceous nanoparticles as surfactant carrier in enhanced oil recovery: a laboratory study, Fuel, 222 (2018) 561–568.
[9] J. Ge, H.-Y. Zhao, H.-W. Zhu, J. Huang, L.-A. Shi, S.-H. Yu, Advanced sorbents for oil-spill cleanup: recent advances and future perspectives, Adv. Mater., 28 (2016) 10459–10490.
[10] A.K. Kota, G. Kwon, W.J. Choi, J.M. Mabry, A. Tuteja, Hygro-responsive membranes for effective oil–water separation, Nat. Commun., 3 (2012) 1025.

[11] A.M. Al-Sabagh, N.G. Kandile, M.R. Noor El-Din, Functions of demulsifiers in the petroleum industry, Sep. Sci. Technol., 46 (2011) 1144–1163.
[12] D.D. Yuan, S.H. Liu, Y.L. Zhang, X. Sui, C.H. Nie, H. Jiang, B.H. Wang, Emulsifying and demulsifying chemistry for enhancing the ClO_2-oxidative separation pilot of ultrastable oil-water emulsions, Desal. Wat. Treat., 142 (2019) 185–192.
[13] S.S. da Silva, O. Chiavone, E.L.D. Neto, E.L. Foletto, Oil removal of oilfield-produced water by induced air flotation using nonionic surfactants, Desal. Wat. Treat., 56 (2015) 1802–1808.
[14] A. Ezzati, E. Gorouhi, T. Mohammadi, Separation of water in oil emulsions using microfiltration, Desalination, 185 (2005) 371–382.
[15] R. Zolfaghari, A. Fakhru'l-Razi, L.C. Abdullah, S.S.E.H. Elnashaie, A. Pendashteh, Demulsification techniques of water-in-oil and oil-in-water emulsions in petroleum industry, Sep. Purif. Technol., 170 (2016) 377–407.
[16] G.J. Hirasaki, C.A. Miller, O.G. Raney, M.K. Poindexter, D.T. Nguyen, J. Hera, Separation of produced emulsions from surfactant enhanced oil recovery processes, Energy Fuels, 25 (2011) 555–561.
[17] D. Nguyen, N. Sadeghi, C. Houston, Chemical interactions and demulsifier characteristics for enhanced oil recovery applications, Energy Fuels, 26 (2012) 2742–2750.
[18] N.H. Abdurahman, Y.M. Rosli, N.H. Azhari, B.A. Hayder, Pipeline transportation of viscous crudes as concentrated oil-in-water emulsions, J. Petrol. Sci. Eng., 90–91 (2012) 139–144.
[19] P. Suemar, E.F. Fonseca, R.C. Coutinho, F. Machado, R. Fontes, L.C. Ferreira, E.L. Lima, P.A. Melo, J.C. Pinto, M. Nele, Quantitative evaluation of the efficiency of water-in-crude-oil emulsion dehydration by electrocoalescence in pilot-plant and full-scale units, Ind. Eng. Chem. Res., 51 (2012) 13423–13437.
[20] C. Carlesi, N.G. Ramirez, D. Carvajal, M.C. Hernandez, D. Fino, Electrochemical treatment of bilge wastewater, Desal. Wat. Treat., 54 (2015) 1556–1562.
[21] M. Fortuny, C.B.Z. Oliveira, R.L.F.V. Melo, M. Nele, R.C.C. Coutinho, A.F. Santos, Effect of salinity, temperature, water content, and pH on the microwave demulsification of crude oil emulsions, Energy Fuels, 21 (2007) 1358–1364.
[22] S. Nii, S. Kikumoto, H. Tokuyama, Quantitative approach to ultrasonic emulsion separation, Ultrason. Sonochem., 16 (2009) 145–149.
[23] X. Luo, J. Cao, H. Gong, H. Yan, L. He, Phase separation technology based on ultrasonic standing waves: a review, Ultrason. Sonochem., 48 (2018) 287–298.
[24] X. Huang, K. Peng, Y. Feng, J. Liu, L. Lu, Separation and characterization of effective demulsifying substances from surface of *Alcaligenes* sp. S-XJ-1 and its application in water-in-kerosene emulsion, Bioresour. Technol., 139 (2013) 257–264.
[25] X. Huang, K. Peng, L. Lu, R. Wang, J. Liu, Carbon source dependence of cell surface composition and demulsifying capability of *Alcaligenes* sp. S-XJ-1, Environ. Sci. Technol., 48 (2014) 3056–3064.
[26] D. Abdessemed, G. Nezzal, R. Ben Aim, Coagulation-adsorption-ultrafiltration for wastewater treatment and reuse, Desalination, 131 (2000) 307–314.
[27] J. Benito, G. Ríos, E. Ortea, E. Fernández, A. Cambiella, C. Pazos, J. Coca, Design and construction of a modular pilot plant for the treatment of oil-containing wastewaters, Desalination, 147 (2002) 5–10.
[28] C. Liu, T.M. Xiao, J. Zhang, L. Zhang, J.L. Yang, M. Zhang, Effect of membrane wettability on membrane fouling and chemical durability of SPG membranes used in a microbubble-aerated biofilm reactor, Sep. Purif. Technol., 127 (2014) 157–164.
[29] M. Karhu, T. Kuokkanen, J. Rämö, M. Mikola, J. Tanskanen, Performance of a commercial industrial-scale UF-based process for treatment of oily wastewaters, J. Environ. Manage., 128 (2013) 413–420.
[30] J. Wang, Y. Zheng, Oil/water mixtures and emulsions separation of stearic acid-functionalized sponge fabricated via a facile one-step coating method, Sep. Purif. Technol., 181 (2017) 183–191.
[31] J. Wang, H. Wang, G. Geng, Highly efficient oil-in-water emulsion and oil layer/water mixture separation based on durably superhydrophobic sponge prepared via a facile route, Mar. Pollut. Bull., 127 (2018) 108–116.
[32] T. Mohammadi, M. Kazemimoghadam, M. Saadabadi, Modeling of membrane fouling and flux decline in reverse osmosis during separation of oil in water emulsions, Desalination, 157 (2003) 369–375.
[33] M. Gryta, K. Karakulski, The application of membrane distillation for the concentration of oil-water emulsions, Desalination, 121 (1999) 23–29.
[34] E. Karimi, S.S. Barekati, A. Raisi, A. Aroujalian, High-flux electrospun polyvinyl alcohol microfiltration nanofiber membranes for treatment of oil water emulsion, Desal. Wat. Treat., 147 (2019) 20–30.
[35] Q.B. Chang, X. Wang, Y.Q. Wang, X.Z. Zhang, S. Cerneaux, J.E. Zhou, Effect of hydrophilic modification with nano-titania and operation modes on the oil-water separation performance of microfiltration membrane, Desal. Wat. Treat., 57 (2016) 4788–4795.
[36] Y.L. Su, Q. Zhao, J.Z. Liu, J.J. Zhao, Y.F. Li, Z.Y. Jiang, Improved oil/water emulsion separation performance of PVC/CPVC blend ultrafiltration membranes by fluorination treatment, Desal. Wat. Treat., 55 (2015) 304–314.
[37] N. Kamoun, M.A. Rodriguez, F. Jamoussi, Ceramic filters for oil emulsion treatments, Desal. Wat. Treat., 57 (2016) 28071–28076.
[38] N. Liu, Q. Zhang, R. Qu, W. Zhang, H. Li, Y. Wei, L. Feng, Nanocomposite deposited membrane for oil-in-water emulsion separation with in situ removal of anionic dyes and surfactants, Langmuir, 33 (2017) 7380–7388.
[39] H.C. Yang, J. Luo, Y. Lv, P. Shen, Z.K. Xu, Surface engineering of polymer membranes via mussel-inspired chemistry, J. Membr. Sci., 483 (2015) 42–59.
[40] W. Wei, M. Sun, L. Zhang, S. Zhao, J. Wu, J. Wang, Underwater oleophobic PTFE membrane for efficient and reusable emulsion separation and the influence of surface wettability and pore size, Sep. Purif. Technol., 189 (2017) 32–39.
[41] W.Y. Lv, Q.Q. Mei, J.L. Xiao, M. Du, Q. Zheng, 3D multiscale superhydrophilic sponges with delicately designed pore size for ultrafast oil/water separation, Adv. Funct. Mater., 27 (2017) 9.
[42] N.M. Kocherginsky, C.L. Tan, W.F. Lu, Demulsification of water-in-oil emulsions via filtration through a hydrophilic polymer membrane, J. Membr. Sci., 220 (2003) 117–128.
[43] K.-Y.A. Lin, Y.-C. Chen, S. Phattarapattamawong, Efficient demulsification of oil-in-water emulsions using a zeolitic imidazolate framework: adsorptive removal of oil droplets from water, J. Colloid Interface Sci., 478 (2016) 97–106.
[44] Z. Wang, G. Liu, S. Huang, In situ generated janus fabrics for the rapid and efficient separation of oil from oil-in-water emulsions, Angew. Chem. Int. Ed., 55 (2016) 14610–14613.
[45] L. Xu, Y. Chen, N. Liu, W. Zhang, Y. Yang, Y. Cao, X. Lin, Y. Wei, L. Feng, Breathing demulsification: a three-dimensional (3D) free-standing superhydrophilic sponge, ACS Appl. Mater. Interfaces, 7 (2015) 22264–22271.
[46] J. Wu, W. Wei, S. Li, Q. Zhong, F. Liu, J. Zheng, J. Wang, The effect of membrane surface charges on demulsification and fouling resistance during emulsion separation, J. Membr. Sci., 563 (2018) 126–133.
[47] H.C. Flemming, Biofilms and environmental protection, Water Sci. Technol., 27 (1993) 1–10.
[48] H.C. Flemming, G. Schaule, T. Griebe, J. Schmitt, A. Tamachkiarowa, Biofouling—the Achilles heel of membrane processes, Desalination, 113 (1997) 215–225.
[49] M. Herzberg, M. Elimelech, Biofouling of reverse osmosis membranes: role of biofilm-enhanced osmotic pressure, J. Membr. Sci., 295 (2007) 11–20.
[50] N. Misdan, A.F. Ismail, N. Hilal, Recent advances in the development of (bio)fouling resistant thin film composite membranes for desalination, Desalination, 380 (2016) 105–111.
[51] J.Y. Wu, C.W. Huang, P.S. Tsai, Preparation of poly[3-(methacryloylamino) propyl] trimethylammonium chloride

coated mesh for oil–water separation, Desal. Wat. Treat., 158 (2019) 301–308.
[52] Z. Xue, S. Wang, L. Lin, L. Chen, M. Liu, L. Feng, L. Jiang, A novel superhydrophilic and underwater superoleophobic hydrogel-coated mesh for oil/water separation, Adv. Mater., 23 (2011) 4270–4273.
[53] S. Chitikela, S.K. Dentel, H.E. Allen, Modified method for the analysis of anionic surfactants as Methylene Blue active substances, Analyst, 120 (1995) 2001–2004.
[54] APHA, AWWA, Standard Methods for the Examination of Water and Wastewater, American Public Health Association, 1989.
[55] D. Coelho, A. Sampaio, C.J.S.M. Silva, H.P. Felgueiras, M.T.P. Amorim, A. Zille, Antibacterial electrospun poly(vinyl alcohol)/enzymatic synthesized poly(catechol) nanofibrous midlayer membrane for ultrafiltration, ACS Appl. Mater. Interfaces, 9 (2017) 33107–33118.
[56] H. Yu, Y. Zhang, J. Zhang, H. Zhang, J. Liu, Preparation and antibacterial property of SiO_2–Ag/PES hybrid ultrafiltration membranes, Desal. Wat. Treat., 51 (2013) 3584–3590.
[57] J. Liu, W. He, P. Li, S. Xia, X. Lu, Z. Liu, P. Yan, T. Tian, Synthesis of graphene oxide-SiO_2 coated mesh film and its properties on oil-water separation and antibacterial activity, Water Sci. Technol., 73 (2016) 1098–1103.
[58] L.F. Jiang, X.M. Kong, Z.C. Lu, S.S. Hou, Preparation of amphoteric polycarboxylate superplasticizers and their performances in cementitious system, J. Appl. Polym. Sci., 132 (2015), https://doi.org/10.1002/app.41348.
[59] D.A. Palacio, B.L. Rivas, B.F. Urbano, Ultrafiltration membranes with three water-soluble polyelectrolyte copolymers to remove ciprofloxacin from aqueous systems, Chem. Eng. J., 351 (2018) 85–93.
[60] T. Hoshika, Y. Nishitani, M. Yoshiyama, W.O. Key, W. Brantley, K.A. Agee, L. Breschi, M. Cadenaro, F.R. Tay, F. Rueggeberg, D.H. Pashley, Effects of quaternary ammonium-methacrylates on the mechanical properties of unfilled resins, Dent. Mater., 30 (2014) 1213–1223.